Gupta, J., Lin, C.-H., and Chen, Q. 2011. "Transport of expiratory droplets in an aircraft cabin," *Indoor Air, 21(1), 3-11.*

Transport of expiratory droplets in an aircraft cabin

Jitendra K. Gupta[a], Chao-Hsin Lin[b], Ph.D., Qingyan Chen[a], Ph.D.

[a] National Air Transportation Center of Excellence for Research in the Intermodal Transport Environment (RITE), School of Mechanical Engineering, Purdue University, West Lafayette, IN 47907-2088, USA

[b] Environmental Control Systems, Boeing Commercial Airplanes, Everett, WA 98203, USA

Corresponding Author: Dr. Qingyan Chen- yanchen@purdue.edu

The droplets exhaled by an index patient with infectious disease such as influenza or Tuberculosis may be the carriers of contagious agents. Indoor environments such as the airliner cabins may be susceptible to infection from such airborne contagious agents. The present investigation computed the transport of the droplets exhaled by the index patient seated in the middle of a seven-row, twin-aisle, fully-occupied cabin using the CFD simulations. The droplets exhaled were from a single cough, a single breath and a 15-s talk of the index patient. The expiratory droplets were tracked by using Lagrangian method and their evaporation was modeled. It was found that the bulk airflow pattern in the cabin played the most important role on the droplet transport. The droplets were contained in the row before, at, and after the index patient within 30 s and dispersed uniformly to all the seven rows in 4 minutes. The total airborne droplet fraction reduced to 48%, 32%, 20%, and 12% after they entered the cabin for 1, 2, 3 and 4 minutes, respectively, due to the ventilation from the environmental control system.

Keywords: Exhalation, CFD, infectious disease, dispersion, particle

Practical Implications: It is critical to predict the risk of airborne infection to take appropriate measures to control, and mitigate the risk. Most of the studies in past either assume a homogenous distribution of contaminants or use steady state conditions. The present study instead provides information on the transient movement of the droplets exhaled by an index passenger in an aircraft cabin. These droplets may contain active contagious agents and can be a potent enough to cause infection. The findings can be used by medical professionals to estimate the spatial and temporal distribution of risk of infection to various passengers in the cabin.

Introduction

Airborne disease transmission during air travel is important (WHO, 1998). This is because passengers seated in an aircraft cabin are high packed and have a long exposure time. More than 20 passengers were infected with Severe Acute Respiratory Syndrome (SARS) during the Air China flight 112 from Hong Kong to Beijing in 2003 (Olsen et al., 2003). Some of the tuberculosis (TB) outbreaks were believed to be caused by in-flight infection transmission as well (Kenyon et al., 1996). Mangili and Gendreau (2005) reviewed the risks of airborne infection spread among the passengers inside aircraft cabins from various respiratory outbreaks and concluded that risk of in-flight infection disease transmission was very high. As more than two

billion people are traveling each year (Gendreau and DeJohn 2002) in commercial flights, possible infection during a flight can easily cause public attention. This investigation was to understand how airborne disease agents could be transported from an infected passenger to fellow passengers.

Research Method

Airborne contagious agents are typically in the droplets generated from coughing, breathing, sneezing, or talking of an infected patient. The droplets are dispersed in the air and then inhaled by a susceptible person. In an aircraft cabin, the airflow from the environmental control system interacts with furnishing and passengers. The airflow and droplet transport in the cabin are three-dimensional and non-uniform (Singh et al., 2002 and Zhang et al., 2009a). To understand how a passenger could become infected, it is essential to study the transport of the agents in the cabin air.

Previous studies have used computer simulations or experimental measurements to determine airborne contaminant transmission in cabins. The experimental measurements can be expensive though they can provide realistic information (Zhang et al., 2007b; Zhang, 2007c; Sze To et al. 2009 and Yan et al., 2009). The computer simulations by Computational Fluid Dynamics (CFD), on the other hand, are inexpensive and more flexible to changes in the boundary conditions compared with the experimental measurements. The CFD simulations can effectively predict airborne contaminant transport in commercial aircraft cabins and the computed results were in reasonable agreement with the experimental data (Wan et al., 2009; Yan et al., 2009 and Zhang et al., 2009a).

There are a number of studies on contaminant transport in cabins (Aboosaidi et al., 1991; Lin et al., 2005a; Lin et al., 2005b; Wan et al., 2009; Zhang et al., 2009a and Yan et al., 2009). Aboosaidi et al. (1991) considered an empty cabin, but Singh et al. (2002) pointed out that the airflow inside the cabin can change significantly if the buoyancy effect from passengers were considered. Lin et al. (2005a and 2005b) provided great insight of airflow in an aircraft cabin. But the flow domain was for 2 rows, which might not sufficient for studying contaminant transport (Olsen et al., 2003). Wan et al. (2009) and Zhang et al. (2009a) studied particle transport in an aircraft cabin while they did not provide information on how the particles were transported in the cabin over time. Zhang et al., (2009a) found that the renormalization group (RNG) k-ε model (Yakhot and Orszag, 1986) can effectively predict the turbulent feature of the airflow in the aircraft cabins. Yan et al. (2009) used tracer gas as a pollutant and found source location to be important for the pollutant transport. However, the study did not consider the details of exhalations/inhalations.

When CFD is used to compute particle transport in an enclosed environment, either Eulerian or Lagrangian method could be used. The Eulerian method is usually used to predict particle concentration distribution (Mazumdar and Chen, 2008 and Yan et al., 2009), while the Lagrangian method to determine particle dispersion pattern (Zhang and Chen 2006; Zhang and Chen 2007d and Wan et al., 2009). Zhang and Chen (2007d) compared the two methods. They found that the Eulerian and Lagrangian approach predictions were similar under steady state. But for the unsteady scenario the predictions using the Lagrangian methods were better than the Eulerian approach.

This investigation used RNG k-ε model with the Lagrangian method for computing particle dispersion in cabin air. The expiratory droplets are volatile and can evaporate

in cabin air (Morawska, 2006). The expiratory droplets consist of liquid and solid matter. The liquid matter was assumed to be volatile and was 90% of the total volume of the droplets (Potter et al., 1963). The droplets were modeled to evaporate if the droplet temperature was higher than the vaporization temperature of the volatile liquid and if it had non-zero volatile matter (mass) in it. The droplet evaporated until it reduced to its non volatile content (residue). The rate of evaporation is given by

$$N_i = k_c (C_{i,s} - C_{i,\infty}) \quad (1)$$

Where

N_i = molar flux of vapor (kgmolm^{-2}s^{-1})

k_c = mass transfer coefficient (m/s), can be obtained using Sherwood relationship (Ranz and Marshall, 1952).

$C_{i,s}$ = vapor concentration at the droplet surface (kgmolm^{-3})

$C_{i,,\infty}$ = vapor concentration in the bulk gas (kgmolm^{-3})

$C_{i,s}$ and $C_{i,,\infty}$ can be obtained using the ideal gas relationship and molar fractions of water vapor.

Zhang (2007c) reviewed the particle deposition studies in indoor environment and have indicated that the particle deposition velocity for the current range of droplet diameter is 10^{-6} to 10^{-4} m/s. The particle loss coefficient for the aircraft cabin for this range comes out to be .01 to 1 (h^{-1}), this is much less than the air exchange rate in the aircraft cabins (25-40 ACH). ACH is defined as the air change per hour. A recent experimental study by Chao et al. (2008) indicated that the particle deposition fraction for this range of droplet diameter was around 10%-20% for 6-12 ACH exchange rates in hospital environment. An experimental study by Sze To et al. (2009) found out about 75% of particles by mass deposits in aircraft cabins. They had around 90% of the particles of size more than 100 microns and they would have higher tendency to deposit. As the particle deposition rate for the droplets of size 0.16 to 12 micron with 25-40 ACH is less than 10%, no deposition on the surfaces was assumed in the current study. Thus, these droplets reflect from the solid surfaces with a low coefficient of restitution (Zhang et al., 2009a). This means that droplet will be stationary when it reaches the wall and thus can only be picked by the bulk airflow.

Therefore, this investigation used CFD simulations with the Lagrangian method for predicting droplet transport in an aircraft cabin. Moreover, this study used the exhalation/inhalation model developed in our previous study (Gupta et al., 2009 and 2010) for coughing, talking and breathing. The second order upwind discretization schemes were used for all the variables except pressure. Pressure discretization was based on PRESTO scheme (FLUENT, 2005). The momentum and pressure equations were coupled through SIMPLE algorithm (Patankar, 1980).

Case Setup

This investigation studied droplet transport due to coughing, breathing, and talking in a seven-row, twin-aisle, fully-occupied cabin as shown in Fig. 1. The index patient sat in the middle as marked by purple color. For talking the passengers in conversation were modeled facing each other. The passenger seats were with an inclination of 15^o to the back from the vertical, as passengers generally prefer to sit in this position for a long flight. A mouth opening of 4 cm^2 and a nose opening of 0.71 cm^2 (for each nostril) was used for each passenger (Gupta et al., 2009 and 2010).

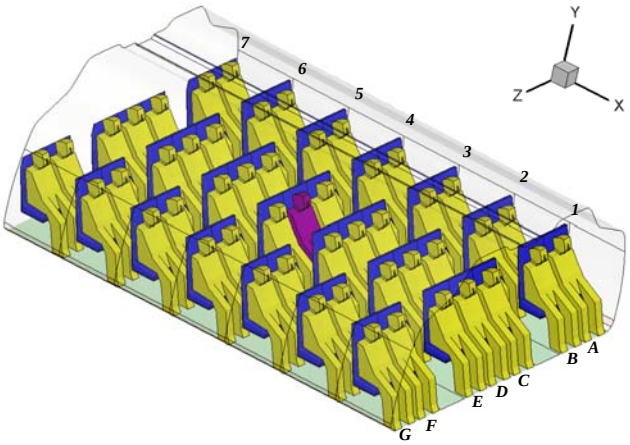

Figure1. Section of a seven-row, twin-aisle, fully occupied cabin used.

The droplet transport simulations used the steady-state airflow pattern in the cabin as the initial condition. The airflow was created by the air supplied from and exhausted by the environmental control systems and the thermal boundary conditions on the cabin surfaces and passengers. Figure 2 and Table 1 show the boundary schematic and conditions. The air exchange rate for the supply inlet conditions was 33.7 ACH.

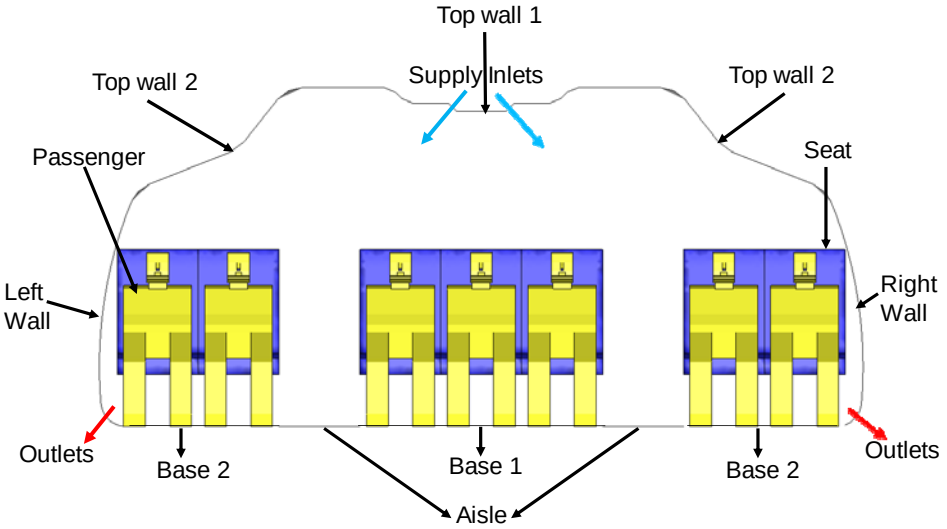

Figure2. Boundary surfaces in the cabin

Table 1 Boundary conditions

Boundary Surface	Velocity	Temperature (°C)	Humidity ratio	Droplet
Human body	No slip	31	zero diffusive flux	Reflect
Seat	No slip	Adiabatic	zero diffusive flux	Reflect
Top Wall1	No slip	23.8	zero diffusive flux	Reflect
Top Wall2	No slip	26.4	zero diffusive flux	Reflect
Left and Right Side wall	No slip	24.5	zero diffusive flux	Reflect
Base 1 (Side)	No slip	24.4	zero diffusive flux	Reflect

Base 2 (center)	No slip	25.1	zero diffusive flux	Reflect
Aisle	No slip	24.1	zero diffusive flux	Reflect
Inlets	2.88 m/s (x=0,y=-0.3,z=±0.95)	19.3	0.003 (20%RH)	Escape
Outlets	Outflow			Escape
Mouth and nose of the infected passenger	-	33 (Hoppe, 1981)	0.007 (50% RH)	Reflect
Mouth of rest of the passenger	-	31	zero diffusive flux	Reflect
Nose of rest of the passenger	No slip (Steady) / Random breath(Unsteady)	31 (Steady)/ 33 (Unsteady)	0.007 (50% RH)	Reflect
Back and front	Periodic			

The boundary conditions and the exhalation jet direction for coughing, breathing and talking processes of the passengers were specified according to our previous study (Gupta et al., 2009 and 2010). The flow boundary conditions at the nose and mouth of the index passenger were different depending on whether he/she was coughing, breathing or talking. For rest of the passengers, the mouth was assumed to be closed all the time except the one who was talking with the index passenger. In real situations all the passengers, including the index passenger will breathe. The passengers can breathe differently, thus an asynchronous (random) breathing pattern was assigned for each passenger to simulate one such case. The random breathing pattern was assigned to these passengers such that every passenger had a random breathing minute volume, breathing frequency and start of the breathing cycle. Figure 3 shows the representative breathing pattern assigned to the passengers in a row.

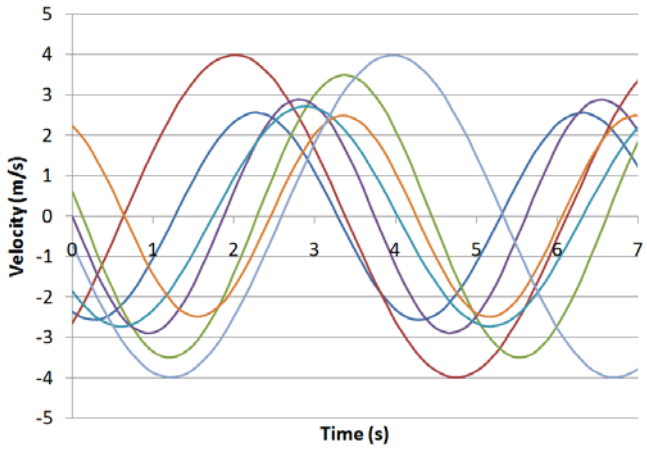

Figure 3. Random breathing distribution provided at the nose of passengers

Figure 4 shows the velocity boundary conditions at the mouth and nose respectively for the infected passenger for the coughing case. It should be noticed that there was no exhalation from the nose during the coughing period and once the coughing process was over there was no exhalation from the mouth while there was an immediate inhalation from nose.

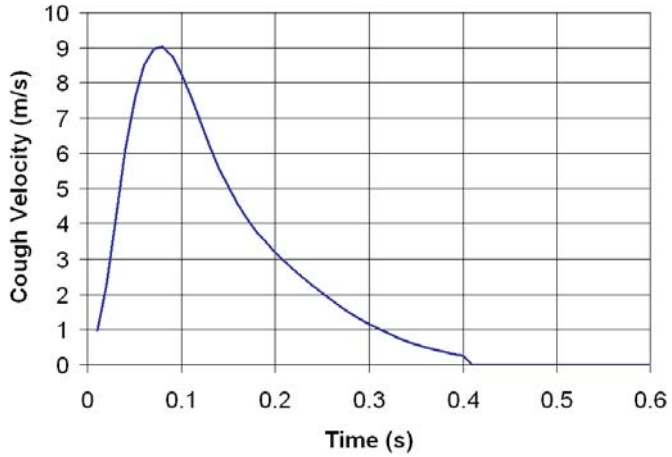

(a)

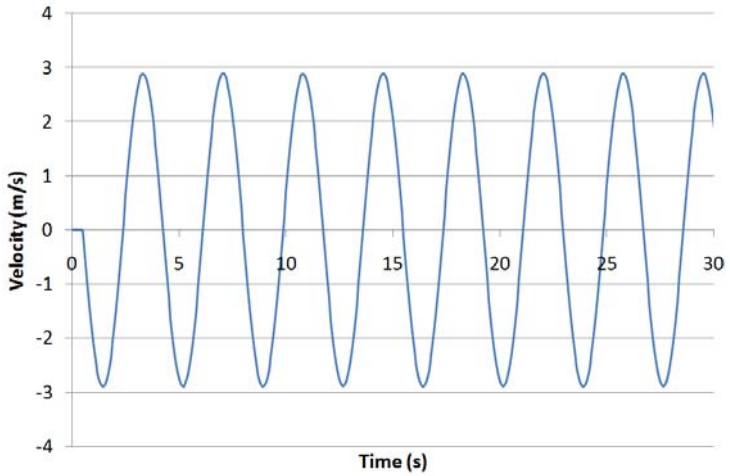

(b)

Figure 4. Flow boundary condition for the index patient at the (a) mouth and (b) nose

The current investigations were performed using mono-dispersed droplets for the coughing, breathing and talking cases. Therefore it was assumed that all the droplets exhaled during a particular exhalation were of one size. A single size droplet and the total amount of droplets exhaled during the exhalation were selected from the literature and used in the simulation. There is a wide range of literature on expiratory droplet size and concentration measurements for coughing, breathing, and talking processes (Duguid, 1946; Fairchild and Stampfer, 1987; Edwards et al., 2004; Yang et al., 2007 and Fabian et al., 2008). There were differences in the finding as these measurements were performed on different subjects using different methods. Yang et al., 2007 found that the average mode size of droplets exhaled during coughing was 8.35 μm, while the droplet concentration was of the order of 10^3 per cm^3. Therefore droplet size of 8.5 μm and concentration of 10^6 per cough (considering the order of volume exhaled during the cough) was used for the current investigation. Fabian et al., 2008 found that the droplets exhaled by the influenza infected subjects were mostly in the range of 0.3 to 0.5 μm. The total droplet concentration ranged from 67 to 8500 particles per liter of air (geometric mean of 724). Fairchild and Stampfer, 1987 and Edwards et al., 2004 also indicated that the amount of droplets exhaled during breathing were of the order of 10^3 per liter. Thus for the breathing simulated in the

current investigation, we obtained 525 droplets exhaled per breath considering 10^3 droplets exhaled per liter. A mean droplet size of 0.4 μm and concentration of 525 per breath was thus used for the breathing exhalation simulations. Duguid, 1946 measured the size distribution of droplets exhaled during talking (counting from 1 -100) but did not quantify the droplet concentration (droplets/cm^3). There was no single dominating size for talking (Duguid, 1946); therefore a mean size (30 μm) was calculated and used in the current investigations. Fairchild and Stampfer found that the droplet concentration exhaled during talking was of the order of 10^3 droplets per liter. Therefore droplet size of 30 μm and concentration of 10^3 droplets per liter, which implies 2250 droplets exhaled during the 15 seconds of talking, was used for the CFD simulations. Table 2 shows the mean droplet diameter and number of droplets used in the study.

Table 2 Droplet size and concentration for various exhalation activities

Exhalation	***Droplet Diameter (μm)***	***Number of droplets***
Coughing	8.5	10^6 per cough
Breathing	0.4	525 per breath
Talking	30	2250 for 15 sec of talk

This investigation performed a grid sensitivity analysis to obtain an optimum grid for the further analysis. A grid with 5 mm size on mouth, nose and face of the passengers, 20 mm size on the rest of the body of the passenger and seats, and 40 mm elsewhere was created. More than 98.5% of the cells had equi-size skew angle of less than 0.7. The width of the each cell was then decreased to half to obtain the finer grid. The number of tetrahedral elements for the coarse and find grids was 1.5 million and 10 million respectively. A comparison of velocities and temperature for the two grids showed similar results and the differences were within 0.07 m/s and 0.6°C respectively. As the differences were low, the coarse grid was used for further analysis.

Results

Our studies on the transient transport of droplets exhaled from coughing, breathing, and talking of the index patient in the cabin used the steady state airflow pattern as the initial condition. Figure 5(a) shows the velocity vectors in a cross section located in front of the index patient and Figures 5(b) and 5(c) in longitudinal sections through the index patient and along the aisle, respectively. The airflow pattern was similar to those obtained by Zhang and Chen (2007a) and Zhang et al. (2009a). The cold air from the supply inlets flowed to the sides along the top wall and a part of it existed through the outlets located at the bottom sides. The other part and the thermal plumes created two large re-circulations in a cross section. The airflow pattern clearly indicates the mixed convection in a cross section. The air velocities at the top, center and window zones (Figure 5 (a)) of the cabin ranged from 0.6 to 0.8 m/s, 0.2 to 0.3 m/s, and 0.3 to 0.4 m/s respectively. It should be noticed that the flow was approximately symmetrical about the center line (longitudinal direction) and the airflow current on the top were strong in the lateral direction. The strong airflow near the vicinity of the passengers as shown in Figure 5(b) was due to the thermal plumes around the human bodies. The air velocities around these passengers ranged from 0.2 to 0.3 m/s (Figure 5 (b)). The airflow was upwards and towards the back. While for the plane along the aisle (Figure 5(c)) the airflow was upwards and was to the front especially in the lower zone (0.2-0.3 m/s).

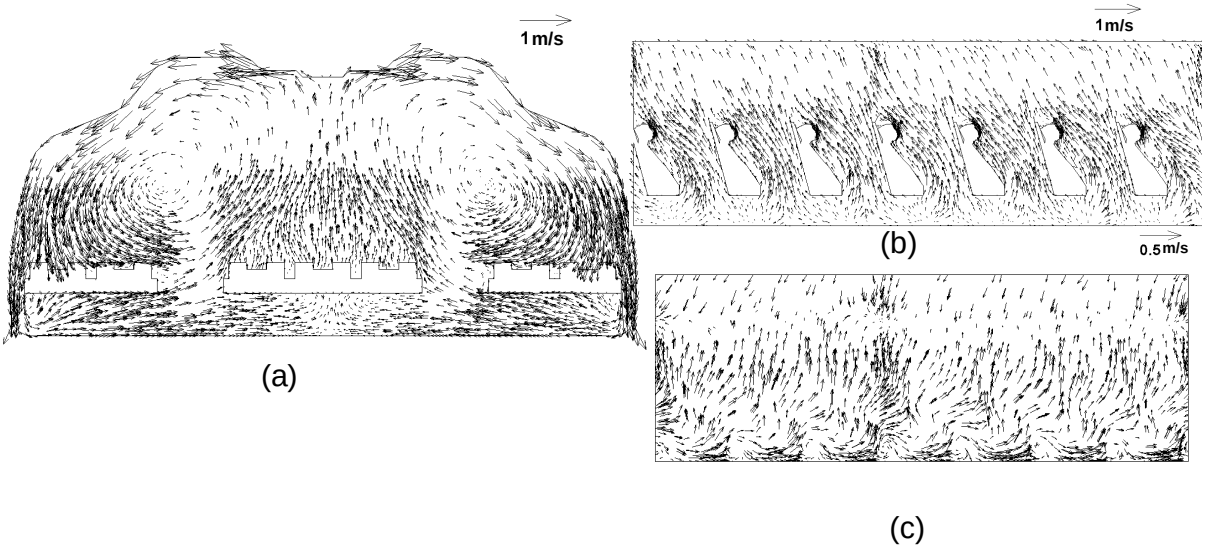

Figure 5. Velocity fields in the cabin on (a) cross section through the index patient (b) longitudinal section through the index patient (c) longitudinal section along the aisle.

Figure 6 shows the change in diameter due to evaporation for the droplets exhaled through coughing, breathing and talking. All these droplets evaporated to their nuclei in less than 0.3 seconds. The droplets with smaller diameter had higher rate of evaporation and evaporated quickly. The droplets generated from breathing were smallest (0.4 μm) and evaporated in 0.005 s. The droplets produced from talking were the largest (30 μm), so they took 0.3 s to evaporate. The time required for the evaporation of these droplets agrees with the finding by Morawska (2006). It should be noticed that none of these droplets evaporated completely because they contained 10% non-volatile matter. The expiratory droplets from coughing, breathing and talking reduced to 4, 0.19, and 14 μm, respectively, after evaporation completed. The diameter of these droplets was small and thus their deposition on the surfaces was minimal.

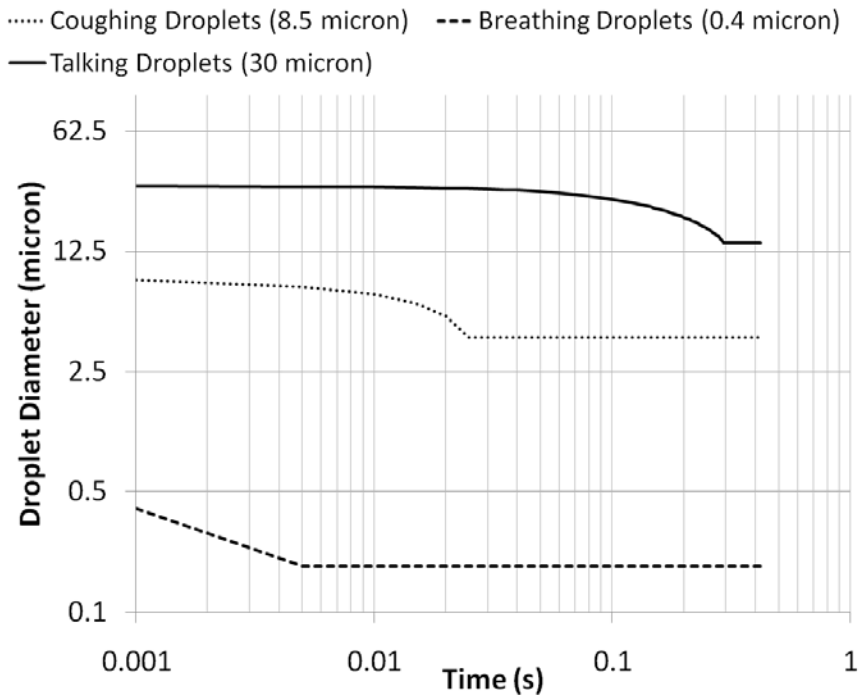

Figure 6. Evaporation of droplets from coughing, breathing and talking

Coughing

Figure 7 shows temporal distributions of the droplets exhaled due to a single cough of the index patient in a perspective and the side view. The droplets shown are 0.001 times the actual number of droplets (1×10^6) contained in a cough. The diameter of the droplets shown in the figure is 1 mm (relative to cabin dimensions), which is two order of magnitude larger than the actual one. This was done to clearly visualize the droplet movement.

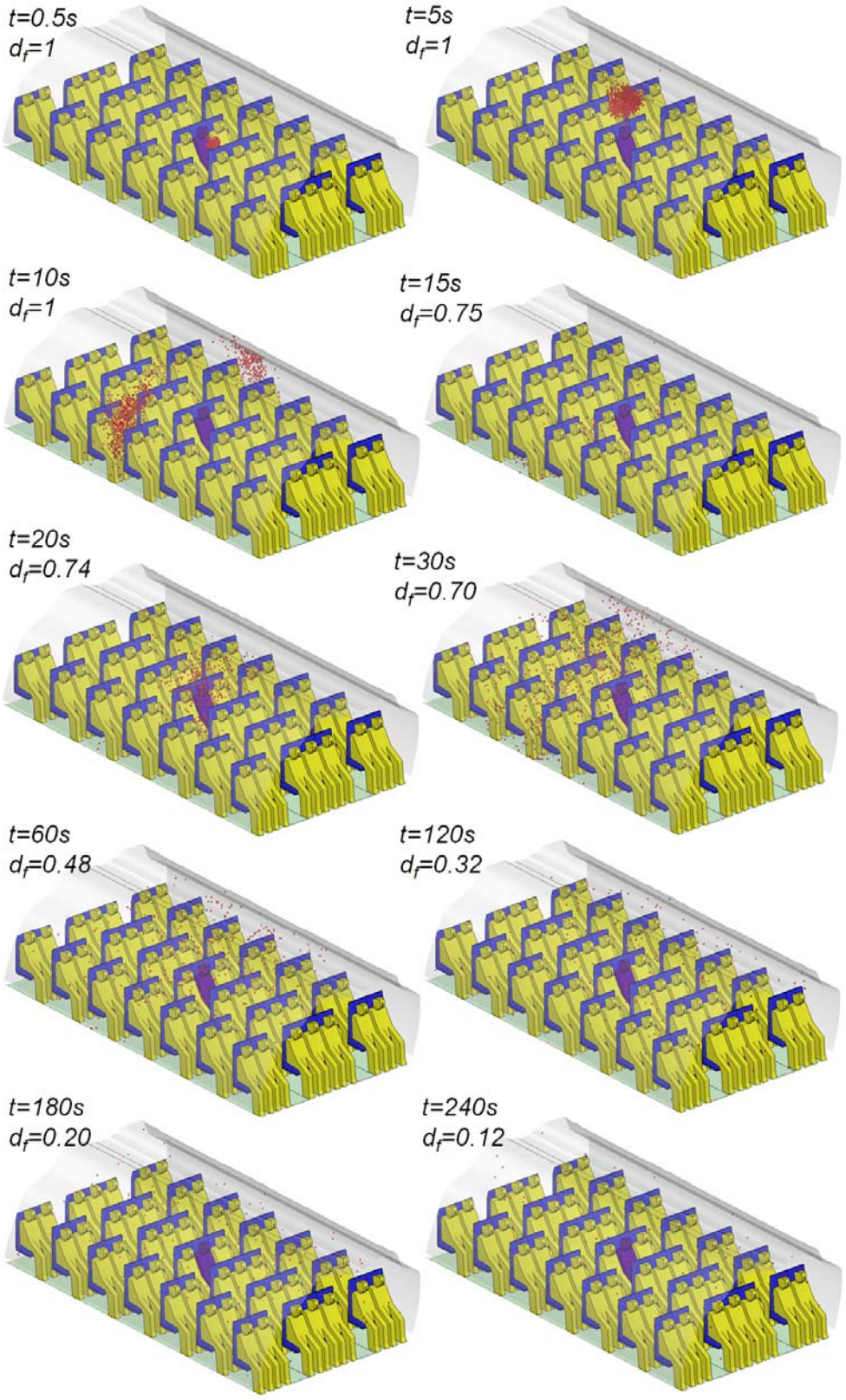
t=0.5s
d_f=1
t=5s
d_f=1
t=10s
d_f=1
t=15s
d_f=0.75
t=20s
d_f=0.74
t=30s
d_f=0.70
t=60s
d_f=0.48
t=120s
d_f=0.32
t=180s
d_f=0.20
t=240s
d_f=0.12

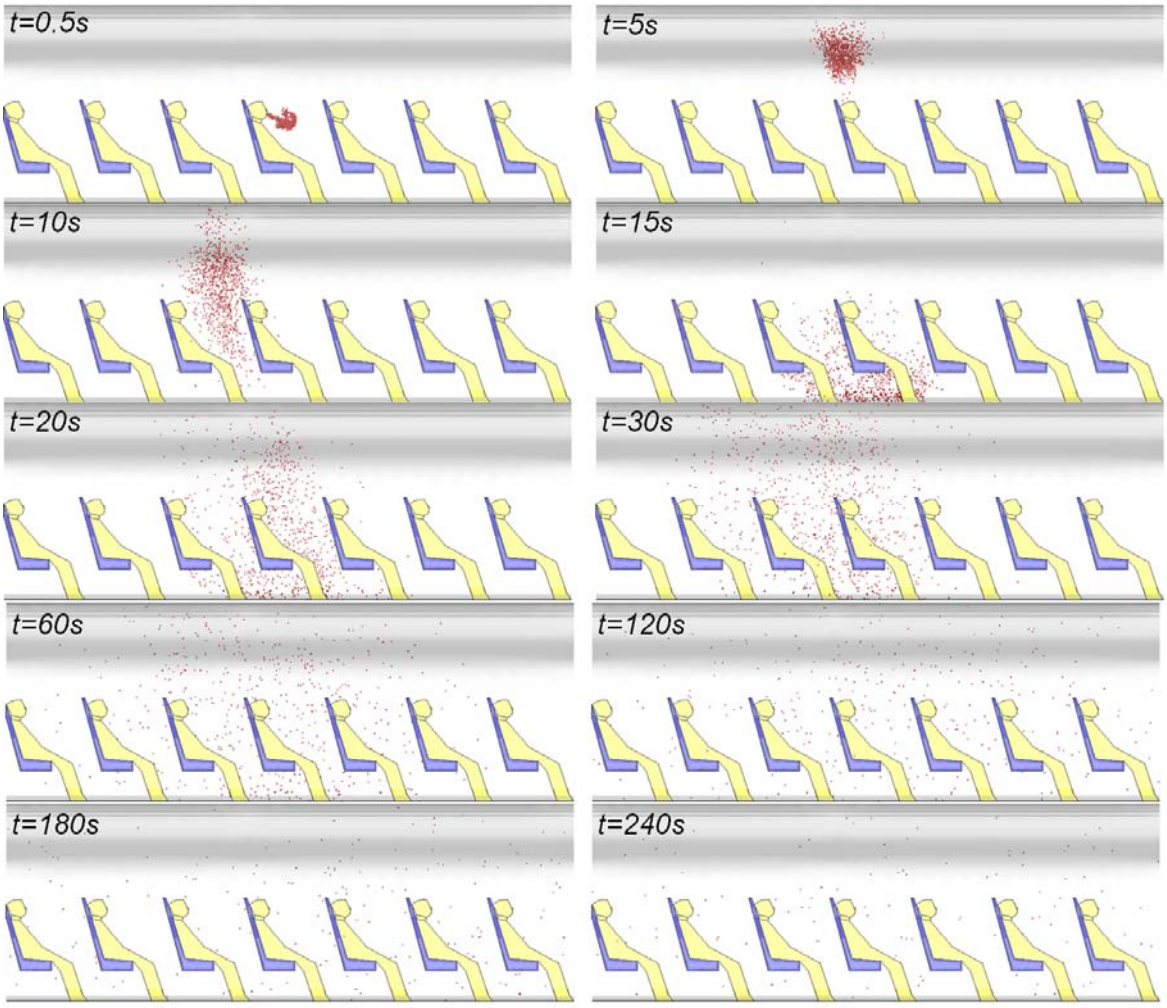

Figure 7. Temporal distributions of droplets due to a single cough from the index patient: (a) a perspective view and (b) the side view

The droplets first followed the air jet caused by the cough, which pushed the droplet cloud down forwards. The simulated cough jet was impulsive in nature with peak velocity of 9m/s. The cough jet penetrated to a distance of about 45 cm axially. The air velocities in this zone decayed to around 0.3 m/s after 0.5 seconds. As the background cabin velocities around the index passenger ranged from 0.2 to 0.3 m/s, the cough expired droplets followed the bulk airflow soon after the cough was over. Gupta et al., 2009 also observed a similar jet behavior. Though the bulk airflow and the cough jet velocities in their case were not exactly the same but the cough penetration during the cough period in the domain was found to agree well. Since the jet momentum was weak, the droplets followed the bulk airflow in the cabin. The side view showed that the droplets moved upwards within 5 s and went towards the backside of the index patient due to the bulk airflow pattern as shown in Figure 5(b). The droplets reached the cabin ceiling and then went to the side walls in 10s due to the jet flow from the environmental control system. The majority of the droplets reached the passengers sitting at the window seats in about 10-12 s. Due to the high droplet concentration and short life of the droplets (pathogens in the droplets may be alive), the passengers seated at these locations (5A, 5G, 4A, and 4G) may have relatively higher risk of infection. The droplets then moved to the lower level of the

cabin because of the re-circulation airflow as shown in Figure 5(a). When the remaining particles came back the proximity of the index patient, it took around 20s. These droplets then dispersed in the air in the proximity of the index patient.

Figure 7(a) also shows the temporal values of the total airborne droplet fraction (d_f), defined as the number of airborne droplets in the cabin over the total amount of droplets exhaled. In 20 s, the d_f become 0.74 (or 74%) that indicates that about 26% of the infectious droplets exhausted from the outlets

These droplets dispersed to all the seven rows in a minute, but most of the droplets were contained to the row in front, at, and behind of the index patient. Thus the risk of infection for the passengers sitting in these rows can be significantly higher than those sitting in the other rows. The d_f reduced to 48%, 32%, 20%, and 12% at t = 1, 2, 3 and 4 minutes, respectively. The delay was slow.

It took 4 weeks to run the 4-minute real-time simulation on the 8-parallel-processor computer cluster. The computing time was very long for such a short section of cabin. As the droplet distribution become rather uniform in 4 minutes, a homogenously mixed condition could be used afterwards.

Breathing

Very similarly, Figure 8 shows the temporal distributions of the droplets exhaled through a single breath from the index patient. The number of droplets shown is $1/3^{rd}$ the actual and the diameter of the droplet shown is 1 mm for better visualization. The droplet number from the breath is 3 to 4 magnitude order smaller than that from the cough.

The index patient started to exhale at t = 1.85 s. Since the jet from the breath was much weaker than the cough, the droplets went upwards very quickly due to the bulk airflow pattern. The weak jet did create a slightly different droplet distribution in the first few seconds, but not very evident. In general, the droplet distributions and the d_f for the breath were similar to those for the cough, but the amount of droplets were much smaller.

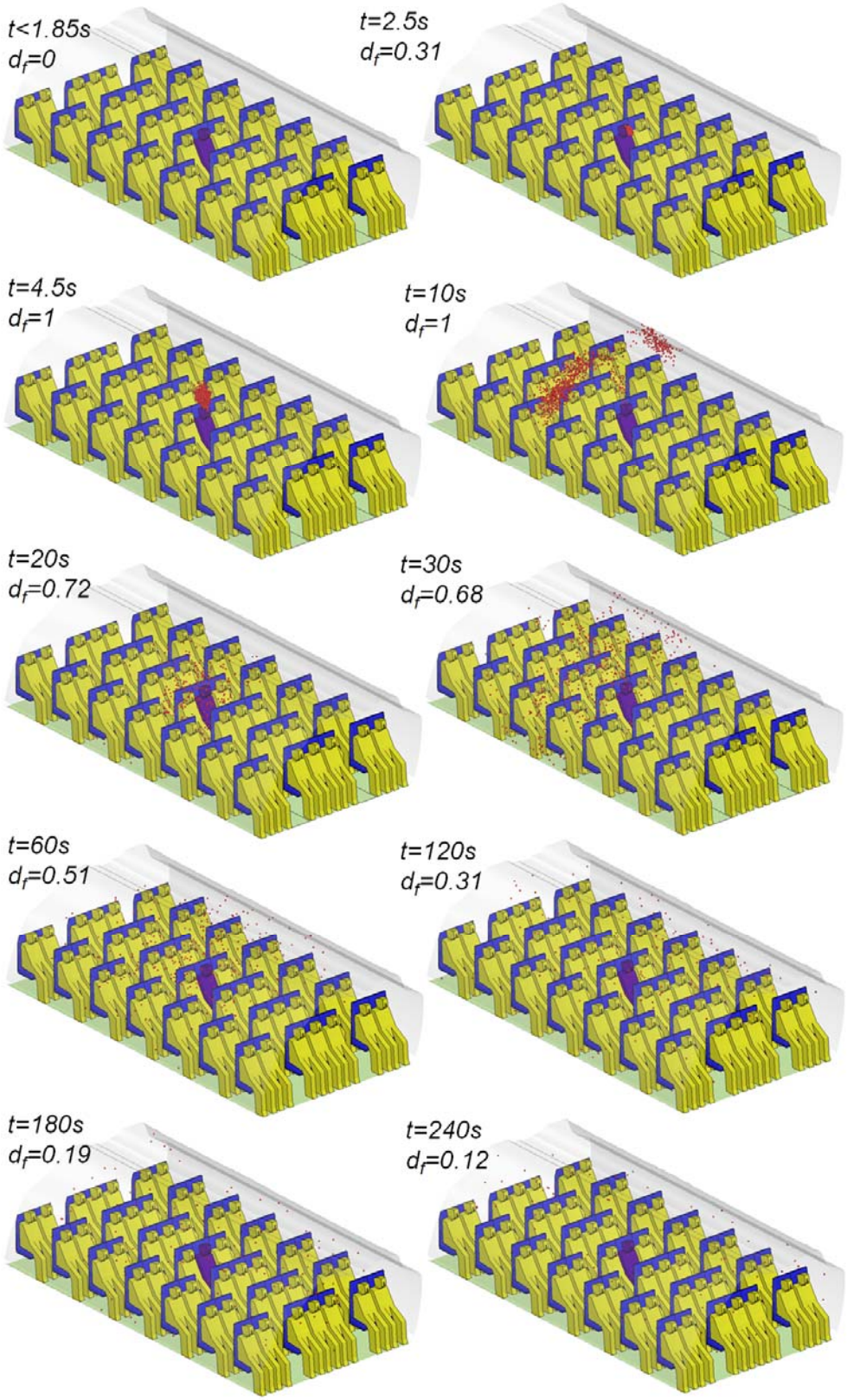
t<1.85s
d_f=0
t=2.5s
d_f=0.31
t=4.5s
d_f=1
t=10s
d_f=1
t=20s
d_f=0.72
t=30s
d_f=0.68
t=60s
d_f=0.51
t=120s
d_f=0.31
t=180s
d_f=0.19
t=240s
d_f=0.12

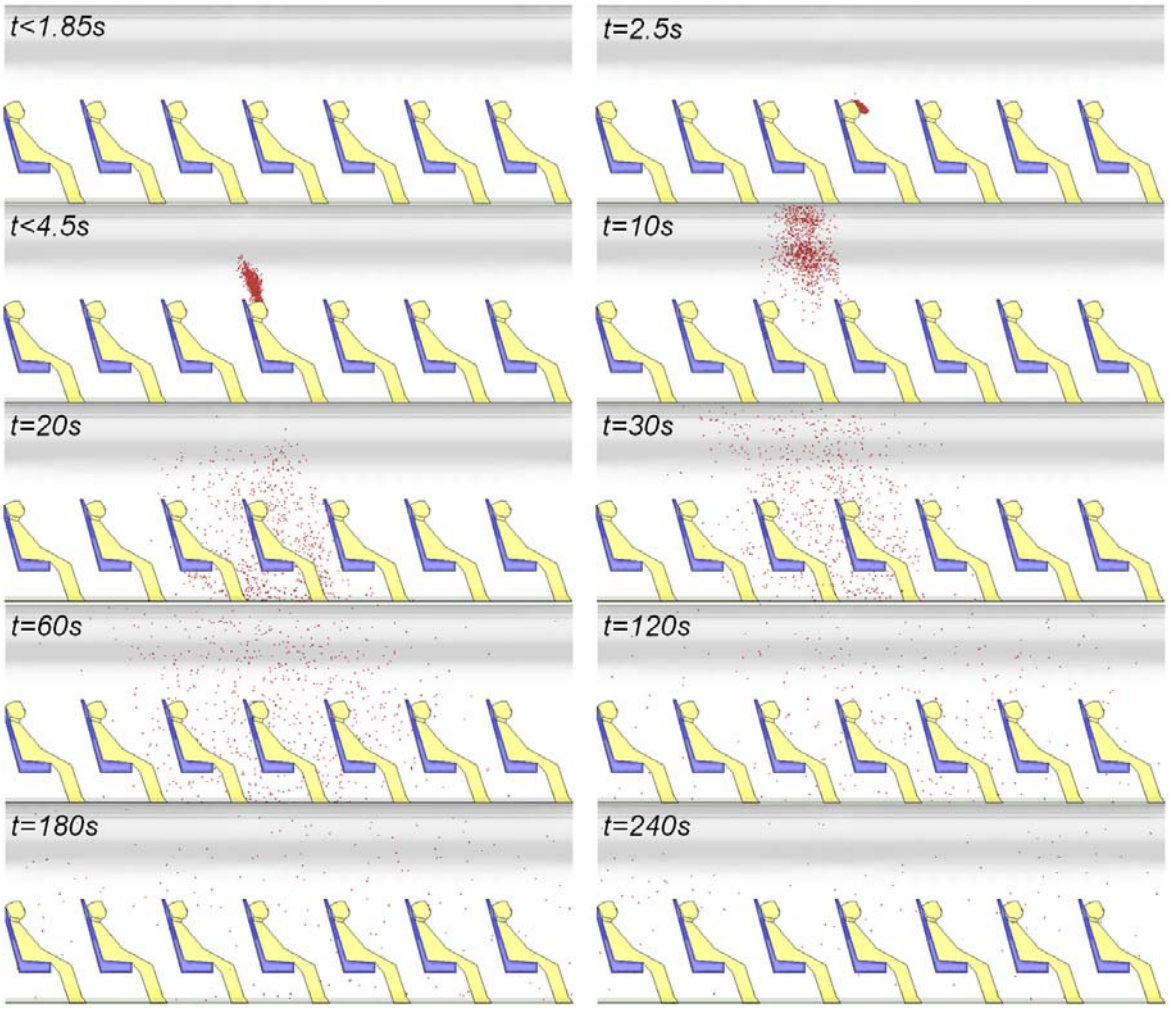

Figure 8. Temporal distributions of droplets due to a single breath from the index patient: (a) a perspective view and (b) the side view

Talking

This investigation also simulated the droplet distributions in the cabin when the index patient talked with the left passenger (4C) for 15 s. Figure 9 show the temporal distributions of the droplets. Similar to the coughing and breathing cases, the number of droplets shown is increased by 2.5 times compared with the actual for better visualization. The index patient was modeled facing to passenger 4C so the droplets exhaled moved to the left side of the index patient.

It is very interesting to see that all the droplets exhaled initially went to the left side of the cabin that was very different from the coughing and breathing case. This is because the head of the index patient turned to the left and the symmetrical bulk airflow brought the droplets to the left side of the cabin. Although some droplets could go to the right side of the cabin at the second recirculation due to diffusion, the amount of the droplets was significantly less than that to the left cabin. Please also note that the talk lasted for 15 s so the droplets were generated continuously during this period. This different source character had some effects on the d_f in initial time. The droplet distribution was uniform in 4 minutes.

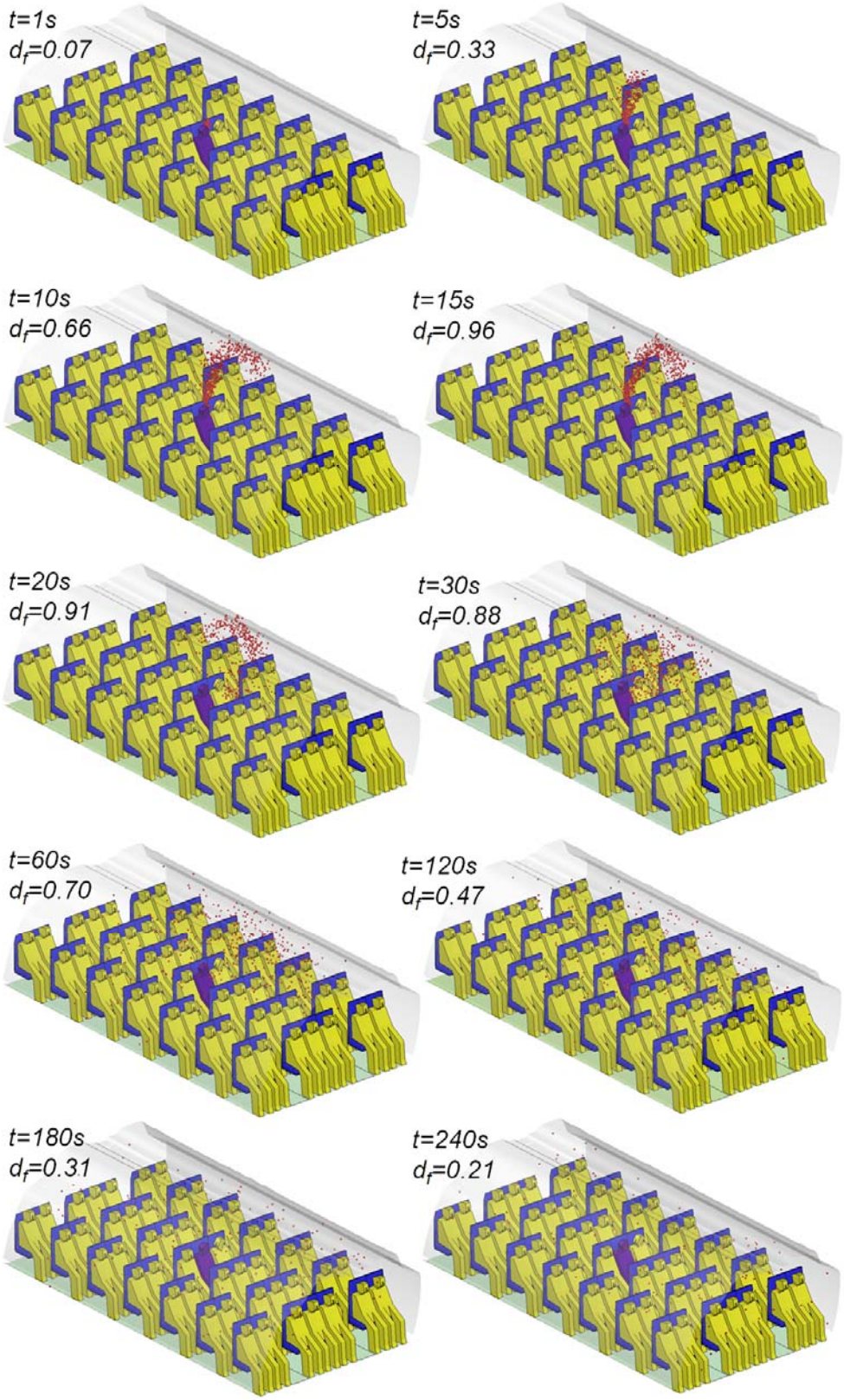
t=1s
d_f=0.07
t=5s
d_f=0.33
t=10s
d_f=0.66
t=15s
d_f=0.96
t=20s
d_f=0.91
t=30s
d_f=0.88
t=60s
d_f=0.70
t=120s
d_f=0.47
t=180s
d_f=0.31
t=240s
d_f=0.21

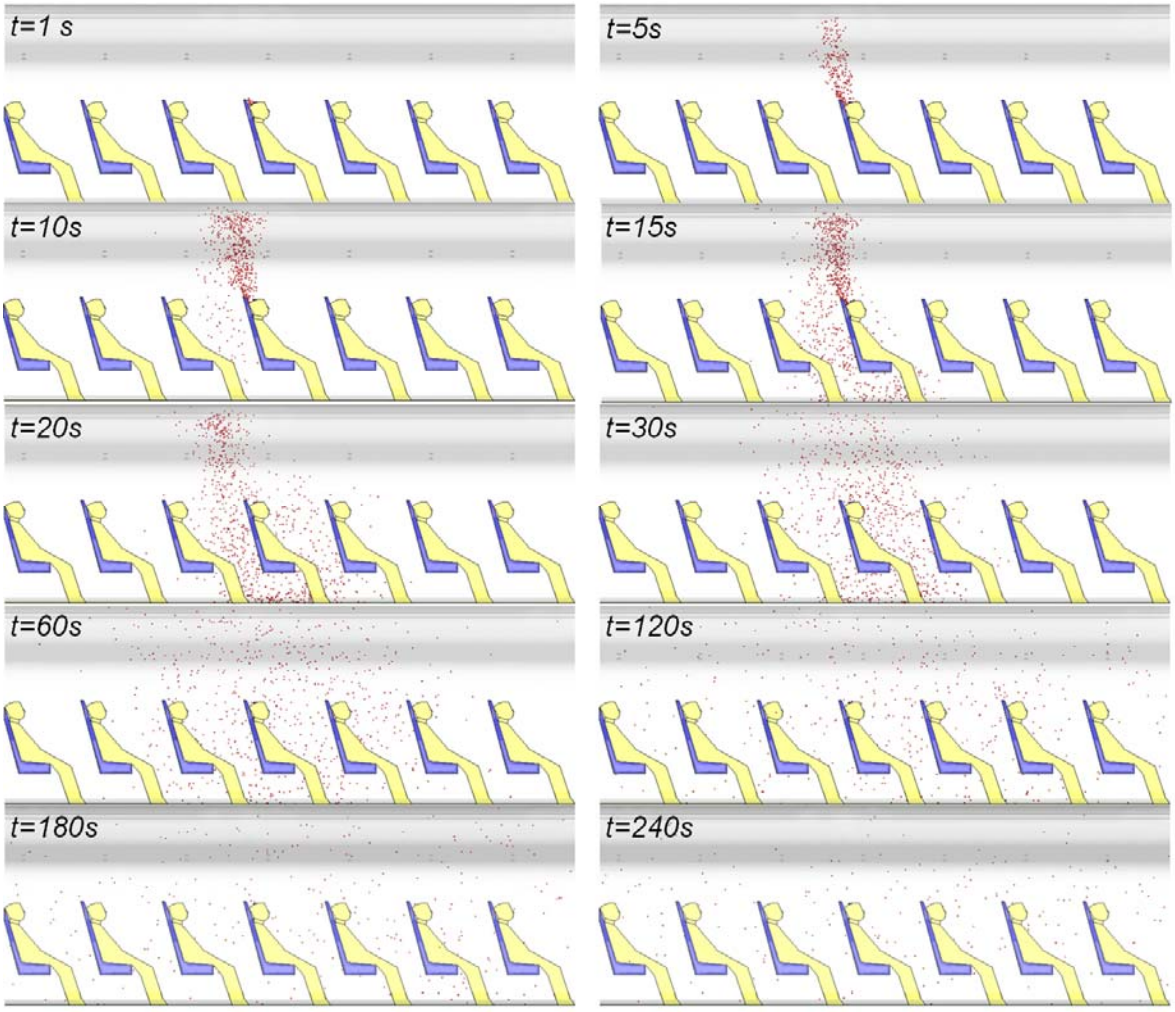

Figure 9. Temporal distributions of droplets due to a 15 s talk from the index patient: (a) a perspective view and (b) the side view

Discussion

The overall flow pattern predicted by the CFD methods was in agreement with the previous literature. The expiratory droplet dispersion was in accordance with the exhaled jet and bulk airflow in the cabin. Zhang et al., 2007b studied the contaminant (scalar) transport in a twin aisle cabin under a steady release. They used CFD methods and validated it against experiments. The contaminant trajectories predicted by them agrees qualitatively with the current investigations. A controlled experimental study is still required for a quantitative validation on the droplet evaporation and dispersion predictions. The validation can aid researchers identify the limitations of the CFD methods used in the current investigations and improve the prediction on the transient transport of expiratory droplets. It is also required to investigate the effect of index passenger location on expiratory droplet dispersion in the cabin.

Moreover, the present study was focused on single exhalation event but the reality is a continuous process with the combination of multiple exhalation events. It is not practical to use the CFD simulations for such a simulation because it would take months of computing time to simulate a one hour flight for an entire cabin. It is required to develop methods to extend the information for realistic flight durations. It is also required to develop methods to quantify the exposure risk to the fellow passengers.

Conclusions

This investigation studied the transport of the expiratory droplets from an index patient seated at the center of a seven-row, twin-aisle, fully occupied aircraft cabin by using a commercial CFD program (FLUENT 2005). The exhalation events studied were a single cough, a single breath, and talk for 15 s by using the models developed in our previous studies (Gupta et al., 2009 and 2010). The simulations were performed for four minutes of real time starting from a steady-state airflow and temperature distribution. The study led to the following conclusions:

The droplets exhaled from the cough of the index patient followed mainly the bulk airflow. The droplet concentration in the vicinity of the passengers reduced over time due to the removal from the outlets and dispersion of the droplets. The total airborne droplet fraction reduced to 48%, 32%, 20%, and 12% after the droplets entered the cabin air for 1, 2, 3 and 4 minutes, respectively. Most of the droplets were transported within one row of the index patient in the first 30 s and then could be transported to the entire seven-row cabin with a uniform droplet distribution in 4 minutes.

The droplets exhaled from the breath of the index patient behaved similarly as those from the cough, but the number was much smaller. The expiratory droplets generated during the talking of the index patient were contained on the left side of the cabin since the patient turned the head to the left.

References

Aboosaidi, F., Warfield, M., and Choudhury, D. (1991) Computational fluid dynamics applications in airplane cabin ventilation system design. Proceedings of Society of Automotive Engineers, 246, 249-258.

Chao, CYH., Wan, MP., and Sze To, GN. (2008) Transport and removal of expiratory droplets in hospital ward environment, Aerosol Science Technology. 42 (5), 377–394.

Duguid, JP. (1946) The size and the duration of air-carriage of respiratory droplets and droplet-nuclei. Journal of Hygiene, 44 (6), 471-479.

Edwards, DA., Man, JC., Brand, P., Katstra, JP., Sommerei, K., Stone, HA., Nardell, E. and Scheuch, G. (2004) Inhaling to mitigate exhaled bioaerosols. Proc Natl Acad Sci USA, 101, 17383-17388.

Fabian, P., McDevitt, JJ., DeHaan, WH., Fung, ROP., Cowling, BJ., Chan, KH., Leung, GM. and Milton, DK. (2008) Influenza Virus in Human Exhaled Breath: An Observational Study. PLoS ONE, 3 (7), e2691.

Fairchild, CI. and Stampfer, JK. (1987) Particle concentration in exhaled breath. Am. Ind. Hyg. Assoc. J, 48(11), 948-949.

Fluent (2005). Fluent 6.2 documentation. Fluent Inc., Lebanon, NH.

Gendreau, MA., and DeJohn, C. (2002) Responding to medical events during commercial airline flights. New England Journal of Medicine, 346(14), 1067-1073.

Gupta, J.K., Lin, C.-H., and Chen, Q. (2009) Flow dynamics and characterization of a cough. Indoor Air, 19 (6), 517-525.

Gupta, J.K., Lin, C.-H., and Chen, Q. (2010) Characterizing exhaled airflow from breathing and talking. Indoor Air, 30 (1), 31-39.

Hoppe, P. (1981) Temperature of Expired Air under Varying Climatic Conditions. International Journal of Biometeor, 25(2), 127-132.

Kenyon, TA., Valway, SE., Ihle, WW., Onorato, IM., and Castro, KG. (1996) Transmission of multidrug resistant mycobacterium tuberculosis during a long airplane flight. New England Journal of Medicine, 334 (15), 933-938.

Lin, CH., Horstman, RH., Ahlers, MF., Sedgwick, LM., Dunn, KH., Topmiller, JL., Bennett, JS., and Wirogo, S. (2005a) Numerical simulation of airflow and airborne pathogen transport in aircraft cabins - Part 1: Numerical simulation of the flow field. ASHRAE Transactions, 111(1), 755-763.

Lin, CH., Horstman, RH., Ahlers, MF., Sedgwick, LM., Dunn, KH., Topmiller, JL., Bennett, JS., and Wirogo, S. (2005b) Numerical simulation of airflow and airborne pathogen transport in aircraft cabins - Part 2: Numerical simulation airborne pathogen transport. ASHRAE Transactions, 111(1), 764-768.

Mangili, A, and Gendreau, MA. (2005) Transmission of infectious disease during commercial air travel. The Lancet, 365 (9463), 989-996.

Mazumdar, S. and Chen, Q. (2008) Influence of cabin conditions on placement and response of contaminant detection sensors in a commercial aircraft. Journal of Environmental Monitoring, 10, 71-81.

Morawska, L. (2006) Droplet fate in indoor environments, or can we prevent the spread of infection? Indoor Air, 16 (5), 335-347.

Olsen, SJ., Chang, HL., Cheung, TY., Tang, AF., Fisk, TL., Ooi, SP., Kuo, HW., Jiang, DD., Chen, KT., Lando, J., Hsu, KH., Chen, TJ., and Dowell, SF. (2003) Transmission of the severe acute respiratory syndrome on aircraft. New England Journal of Medicine, 349(25), 2416-2422.

Patankar, SV. (1980) *Numerical Heat Transfer and Fluid Flow*. Hemisphere, Washington, DC.

Potter, JL., Matthews, LW., Lemm, J. and Spector, S. (1963) Human Pulmonary secretions in Health and disease. Ann. N. Y. Acad. Sci. 106, 692-697.

Ranz, WE. and Marshall, WR., Jr. (1952) Evaporation from Drops, Part I. Chem. Eng. Prog., 48(3):141-146.

Singh, A., Hosni, M., and Horstman, R. (2002) Numerical simulation of airflow in an aircraft cabin section. ASHRAE Transactions, 108(1), 1005-1013.

Sze To, GN., Wan, MP., Chao, CYH., Fang, L., and Melikov, A. (2009). Experimental Study of Dispersion and Deposition of Expiratory Aerosols in

Aircraft Cabins and Impact on Infectious Disease Transmission, Aerosol Science Technology. 43 (5), 466-485.

Wan, MP., Sze To, GN., Chao, CYH., Fang, L. and Melikov, A. (2009) Modeling the Fate of Expiratory Aerosols and the Associated Infection Risk in an Aircraft Cabin Environment. Aerosol Science and Technology, 43(4), 322-343

World Health Organization. (1998) Tuberculosis and air travel: guidelines for prevention and control. WHO Doc, WHO/TB98, 256, 1–45.

Yakhot, V. and Orszag, SA. (1986) Renormalization group analysis of turbulence. Journal of Scientific Computing, 1, 3-51.

Yan, W., Zhang, Y., Sun, Y., and Li, D. (2009) Experimental and CFD study of unsteady airborne pollutant transport within an aircraft cabin mock-up. Building and Environment, 44(1), 34-43

Yang, S., Lee, GWM., Chen CM., WU, CC., and Yu, KP. (2007) The size and concentration of droplets generated by coughing in Human Subjects. Journal of Aerosol Medicine, 20(4), 484-494.

Zhang, T. and Chen, Q. (2007a) Identification of contaminant sources in enclosed spaces by a single sensor, Indoor Air, 17(6), 439-449

Zhang, T., Chen, Q.and Lin, C.-H. (2007b) Optimal sensor placement for airborne contaminant detection in an aircraft cabin. HVAC&R Research, 13(5), 683-696

Zhang, Z. and Chen, Q. (2006) Experimental measurements and numerical simulations of particle transport and distribution in ventilated rooms. Atmospheric Environment, 40(18), 3396-3408.

Zhang, Z. (2007c) Modeling of airflow and contaminant transport in enclosed environments. Ph.D. Thesis. Purdue University.

Zhang, Z. and Chen, Q. (2007d) Comparison of the Eulerian and Lagrangian methods for predicting particle transport in enclosed spaces. Atmospheric Environment, 41(25), 5236-5248.

Zhang, Z., Chen, X., Mazumdar, S., Zhang, T., and Chen, Q. (2009a) Experimental and numerical investigation of airflow and contaminant transport in an airliner cabin mockup. Building and Environment, 44(1), 85-94.